DISCUSSION

This study is the first, to our knowledge, to investigate myosin cross-bridge activity in a heart in a living body. As stated in the Introduction, it is usually difficult to study murine, especially mouse, cardiac muscle in an isolated specimen under conditions that very closely match physiological. The technique here enables one to investigate mouse cardiac muscle under the most physiological condition, opening a way to study cardiac muscle functions of transgenic mice with x-ray diffraction.

The (1,0) lattice spacing observed in this study (37.2 nm in diastole) is close to that reported in an isolated rat heart with saline perfusion (12), as well as in an isolated intact rat papillary muscle at a sarcomere length of 2.1 μm (7). If we assume that a mouse heart in vivo has the same sarcomere length-lattice spacing relation as an isolated rat papillary muscle, the working range of sarcomere length is between 1.9 and 2.1 μm. On the other hand, a much larger lattice spacing has been reported in a thoractomized rat (13). This may be due to a change in osmolarity which is caused by exposure of the circulatory system to the air. Although the open-chest model of rat has the advantage that pressure and volume of left ventricle can be measured easily during the x-ray measurement, it may be too invasive to study the true physiological state of the heart. The present closed-chest method and the open-chest method should be regarded complementary. A lattice spacing of 34 nm was reported in isolated intact rat trabeculae at a sarcomere length of 2.2 μm (16), which is smaller than the present value. Lattice spacing may be important in cardiac muscle because the distance between myofilaments may affect the contractile tension and play a role in Frank-Starling's law. Previous studies to examine the effect of lattice spacing on tension development were made in skinned fibers which had a (1,0) spacing >40 nm (17,18). It is desirable to investigate the effect at smaller lattice spacings, which are more physiological.

The intensity ratios in diastole and systole found in this study are generally similar to those in previous studies. It has been reported that more cross-bridges are formed in heart muscle preparations that are perfused by blood than in those perfused by saline (9). However, comparison of the results on saline-perfused rat heart (12), on blood-perfused rat heart (13), and from this study on mouse heart under the normal condition shows only small differences. Since the early studies required many contractions to record an x-ray diffraction pattern on a photographic film, deterioration of the sample was probably the major cause of low contractility observed in previous studies on saline-perfused specimens.

In isolated cardiac muscles, it has been found that adrenergic β-stimulation enhances the contractile force and makes both tension development and relaxation faster. This is explained by acceleration of calcium uptake (through phosphorylation of phospholamban) and reduction of the binding affinity of troponin-C to calcium (through phosphorylation of troponin-I) (2–4). These lead to faster development of tension, larger twitch tension, and faster decline of tension in cardiac muscle. In this study, the shorter half-time of reduction in the intensity ratio shows a faster formation of cross-bridges with β-stimulation and the lower minimum intensity ratio shows that more cross-bridges are formed. Although the change in the intensity ratio during relaxation was not clearly accelerated, β-stimulation shortened the half-relaxation time of the lattice spacing. These results demonstrate that the changes of contractile properties previously observed in isolated muscle are actually taking place in a heart muscle in vivo.

In this study, the blood pressure and the amount of myosin cross-bridge formation was increased by dobutamine infusion. On the other hand, the heart rate did not change, indicating that the effects of dobutamine stress were modest. Under this condition, the most interesting finding is that β-adrenergic stimulation does not affect the end-diastolic state. Especially, the lattice spacing at end-diastole was unchanged (Fig. 5 *b*). Since the lattice spacing is related to sarcomere length, this suggests that the left ventricular volume at end-diastole was unaffected. The elevation of blood pressure by β-stimulation was simply due to recruitment of more cross-bridges in cardiac muscle of the free wall. The Frank-Starling mechanism, which would be relevant if the end-diastolic volume were larger and the sarcomere length longer, did not play a major role.

By assuming that all myosin cross-bridges are in the vicinity of the thick filaments in a resting state and that all are bound to the thin filaments in the rigor state, it is possible to calculate the fraction of cross-bridges that are transferred to the vicinity of the thin filaments during contraction (see Methods). In canine cardiac muscle, the resting (quiescent) state may not be the same as the diastolic state (9). However, in rat heart muscle, no such evidence has been found. Thus, the diastolic ratio (the first frame in Fig. 5 *a*) is taken as the resting value. Then, the peak cross-bridge mass transfer ratio under the normal condition is 56%, which increases to 74% by dobutamine infusion. The increase is by 34%, whereas the systemic blood pressure increased by 16%. If we take the resting ratio as an average of those in the absence and presence of dobutamine (2.23), the increase is by 26%. In both cases, the increase in the mass transfer ratio is larger than that in the systemic blood pressure. Since the mass transfer ratio with the β-stimulation (75%) is close to the maximum level observed in tetanus of frog skeletal muscle, the major fraction of cross-bridges is recruited for contraction. Thus, even at this modest level of stress that causes an increase in blood pressure but not in heart rate, most of the potential cross-bridge attachments have been made with few in reserve in the β-stimulated heart.

Weisberg and Winegrad (19) showed by electron microscopy that the heads of the α-isoform of myosin heavy chain are more extended from the backbone of the filament when C-protein was phosphorylated by protein kinase A. Since the

α-isoform is dominant in adult mouse ventricle (20) and β-stimulation causes C-protein phosphorylation (1,3,6), a change in the equatorial intensity ratio is expected. Although the results here do not support this observation, more studies at higher dobutamine stress are needed to clarify the effects of C-protein phosphorylation on the behavior of myosin heads.

The experiments were made with the approval of the SPring-8 Program Review Committee (2002B0142-NL2-np, 2003A0079-NL2-np, 2003B0015-NL3-np, 2004B0319-NL3-np, 2005A0455-NL3-np).

This work was supported by a 2002-2004 Research Grant for Cardiomyopathy (14162201-00) from the Ministry of Health, Welfare, and Labor of Japan and by grants from Uehara Memorial Foundation and the Shimabara Science Promotion Foundation.

REFERENCES

1. Jeacocke, S. A., and P. J. England. 1980. Phosphorylation of a myofibrillar protein of Mr 150 000 in perfused rat heart, and the tentative identification of this as C-protein. *FEBS Lett.* 122:129–132.
2. Kranias, E. G., and R. J. Solaro. 1982. Phosphorylation of troponin I and phospholamban during catecholamine stimulation of rabbit heart. *Nature*. 298:182–184.
3. Garvey, J. L., E. G. Kranias, and R. J. Solaro. 1988. Phosphorylation of C-protein, troponin I and phospholamban in isolated rabbit hearts. *Biochem. J.* 249:709–714.
4. Sulakhe, P. V., and X. T. Vo. 1995. Regulation of phospholamban and troponin-I phosphorylation in the intact rat cardiomyocytes by adrenergic and cholinergic stimuli: roles of cyclic nucleotides, calcium, protein kinases and phosphatases and depolarization. *Mol. Cell. Biochem.* 149–150:103–126.
5. Kentish, J. C., D. T. McCloskey, J. Layland, S. Palmer, J. M. Leiden, A. F. Martin, and R. J. Solaro. 2001. Phosphorylation of troponin I by protein kinase A accelerates relaxation and crossbridge cycle kinetics in mouse ventricular muscle. *Circ. Res.* 88:1059–1065.
6. Hartzell, H. C., and L. Titus. 1982. Effects of cholinergic and adrenergic agonists on phosphorylation of a 165,000-dalton myofibrillar protein in intact cardiac muscle. *J. Biol. Chem.* 257:2111–2120.
7. Yagi, N., H. Okuyama, H. Toyota, J. Araki, J. Shimizu, G. Iribe, K. Nakamura, S. Mohri, K. Tsujioka, H. Suga, and F. Kajiya. 2004. Sarcomere-length dependence of lattice volume and radial mass transfer of myosin cross-bridges in rat papillary muscle. *Pflugers Arch.* 445:238–245.
8. Matsubara, I., N. Yagi, D. W. Maughan, Y. Saeki, and Y. Amemiya. 1989. X-ray diffraction study on heart muscle during contraction. *In* Muscle Energetics. R. J. Paul, G. Elzinga, and K. Yamada, editors. Alan T. Liss, New York. 481–486.
9. Matsubara, I. 1980. X-ray diffraction studies on the heart. *Annu. Rev. Biophys. Bioeng.* 9:81–105.
10. Haselgrove, J. C., and H. E. Huxley. 1973. X-ray evidence for radial cross-bridge movement and for the sliding filament model in actively contracting skeletal muscle. *J. Mol. Biol.* 77:549–568.
11. Huxley, H. E., R. M. Simmons, A. R. Faruqi, M. Kress, J. Bordas, and M. H. J. Koch. 1983. Changes in the x-ray reflections from contracting muscle during rapid mechanical transients and their structural implications. *J. Mol. Biol.* 169:469–506.
12. Yagi, N., J. Shimizu, S. Mohri, J. Araki, H. Nakajima, Y. Okumura, H. Toyota, T. Morimoto, Y. Morizane, M. Kurusu, T. Miura, K. Hashimoto, K. Tsujioka, H. Suga, and F. Kajiya. 2004. X-ray diffraction from a left ventricular wall of rat heart. *Biophys. J.* 86:2286–2294.
13. Pearson, J. T., M. Shirai, H. Ito, N. Tokunaga, H. Tsuchimochi, N. Nishiura, D. O. Schwenke, H. Ishibashi-Ueda, R. Akiyama, H. Mori, H. Kangawa, H. Suga, and N. Yagi. 2004. In situ measurements of crossbridge dynamics and lattice spacing in rat hearts by x-ray diffraction: sensitivity to regional ischemia. *Circulation.* 109:2983–2986.
14. Inoue, K., T. Oka, T. Suzuki, N. Yagi, K. Takeshita, S. Goto, and T. Ishikawa. 2001. Present status of high flux beamline (BL40XU) at SPring-8. *Nucl. Instrum. Meth. A.* 467–468:674–677.
15. Amemiya, Y., K. Ito, N. Yagi, Y. Asano, K. Wakabayashi, T. Ueki, and T. Endo. 1995. Large-aperture TV detector with a beryllium-windowed image intensifier for x-ray diffraction. *Rev. Sci. Instrum.* 66:2290–2294.
16. Irving, T. C., J. Konhilas, D. Perry, R. F. Fischetti, and P. P. de Tombe. 2000. Myofilament lattice spacing as a function of sarcomere length in isolated rat myocardium. *Am. J. Physiol.* 279:H2568–H2573.
17. Konhilas, J. P., T. C. Irving, and P. P. de Tombe. 2002. Myofilament calcium sensitivity in skinned rat cardiac trabeculae: role of interfilament spacing. *Circ. Res.* 90:59–65.
18. Wang, Y. P., and F. Fuchs. 1995. Osmotic compression of skinned cardiac and skeletal muscle bundles: effects on force generation, Ca^{2+} sensitivity and Ca^{2+} binding. *J. Mol. Cell. Cardiol.* 27:1235–1244.
19. Weisberg, A., and S. Winegrad. 1998. Relation between crossbridge structure and actomyosin ATPase activity in rat heart. *Circ. Res.* 83: 60–72.
20. Lyons, G. E., S. Schiaffino, D. Sassoon, P. Barton, and M. Buckingham. 1990. Developmental regulation of myosin gene expression in mouse cardiac muscle. *J. Cell Biol.* 111:2427–2436.

Research Paper

Journal of Vascular Research

J Vasc Res 2006;43:131–138
DOI: 10.1159/000090132

Received: March 28, 2005
Accepted after revision: September 23, 2005
Published online: December 7, 2005

Endothelial Urocortin Has Potent Antioxidative Properties and Is Upregulated by Inflammatory Cytokines and Pitavastatin

Tomoyuki Honjo[a] Nobutaka Inoue[a] Rio Shiraki[a] Seiichi Kobayashi[a]
Kazunori Otsui[a] Motonori Takahashi[a] Ken-ichi Hirata[a]
Seinosuke Kawashima[a] Hiroshi Yokozaki[b] Mitsuhiro Yokoyama[a]

[a]Division of Cardiovascular and Respiratory Medicine, Department of Internal Medicine, and [b]Division of Surgical Pathology, Department of Biological Informatics, Kobe University Graduate School of Medicine, Kobe, Japan

Key Words
Endothelium · Oxidative stress · HMG-CoA reductase inhibitors

Abstract
Background: Urocortin, a neuropeptide discovered in the midbrain, is a member of the corticotropin-releasing factor family and is expressed in heart tissues. Urocortin exerts potent cardioprotective effects under various pathological conditions including ischemia/reperfusion. However, the regulation and function of vascular urocortin are unknown. ***Methods and Results:*** Immunohistochemistry showed definitive expression of urocortin in endothelial cells of coronary large arteries and microvessels from autopsied hearts. RT-PCR confirmed the expression of urocortin in human umbilical vein endothelial cells (HUVECs). Urocortin (10^{-8} *M*) potently suppressed the generation of angiotensin II-induced reactive oxygen species (ROS) in HUVECs. Tumor necrosis factor-α and interferon-γ increased the urocortin mRNA levels and its release from HUVECs. Incubation with pitavastatin (0.1–3.0 μ*M*) significantly increased the urocortin mRNA levels and its release from HUVECs. Furthermore, treatment with pitavastatin (2 mg/day) for 4 weeks increased the serum urocortin level from 11.0 ± 6.5 to 16.4 ± 7.3 ng/ml in healthy volunteers. ***Conclusion:*** Endothelial urocortin was upregulated by inflammatory cytokines and pitavastatin and suppressed ROS production in endothelial cells. Treatment with pitavastatin increased the serum urocortin level in human subjects. Thus, endothelial urocortin might protect cardiomyocytes in inflammatory lesions. Urocortin might partly explain the mechanisms of various pleiotropic effects of statins.

Introduction

Urocortin is a 40-amino-acid peptide originally discovered in the rat midbrain and a member of the corticotropin-releasing factor (CRF) family [1]. Human urocortin is expressed not only in the central nervous system, such as in the pituitary [2] and brain [3], but also in various peripheral tissues, including the placenta [4], gastrointestinal tract [5], synovial tissue [6], lymphocytes [7], adipose tissue [8] and heart [9]. These findings suggest that urocortin has some pathophysiologic roles in these peripheral tissues. Especially in the heart, exogenous administration of urocortin induces cardiac inotropic ef-

KARGER
Fax +41 61 306 12 34
E-Mail karger@karger.ch
www.karger.com

1018–1172/06/0432–0131$23.50/0

Accessible online at:
www.karger.com/jvr

Dr. Nobutaka Inoue
Division of Cardiovascular and Respiratory Medicine, Department of Internal Medicine
Kobe University Graduate School of Medicine
7-5-2 Kusunoki-cho, Chuo-ku, Kobe 650-0017 (Japan)
Tel. +81 78 382 5846, Fax +81 78 382 5859, E-Mail nobutaka@ri.nevc.go.jp

fects and coronary vasodilation [10–12]. Moreover, it was reported that exogenous urocortin has potent protective effects on myocardial cells during ischemia. For example, urocortin increases the survival of cultured cardiac cells exposed to ischemia and also rescues the infarct area of rat heart during ischemia/reperfusion [13–17].

The actions of the CRF family peptides are mediated by at least two types of G-protein-coupled receptors, CRF-R1 and CRF-R2 [1]. CRF-R2 exists in three alternative spliced forms, i.e., CRF-R2α, R2β, and R2γ. CRF-R2 is expressed in the cardiovascular system [18, 19], and has higher affinity for urocortin than CRF. Wiley et al. [19] reported that urocortin produced a potent and sustained vasodilator response in isolated human internal mammary artery. The coexpression of CRF-R2 with its preferred urocortin ligand in the heart suggests that urocortin-induced cardioprotective effects are likely mediated by CRF-R2 in an autocrine/paracrine manner [20]. Recently, Florio et al. [21] reported that urocortin is expressed in vessel walls. Furthermore, previous investigations demonstrated that CRF-R2 exists in cultured human umbilical vein endothelial cells (HUVECs) [22]. However, the vascular action of urocortin and its regulation remain unknown.

On the other hand, there is accumulating evidence that besides its potent lipid-lowering effect, HMG-CoA reductase inhibitors have pleiotropic effects such as anti-inflammatory [25, 26], anti-proliferative and anti-oxidative effects [27]. These drugs improve endothelial dysfunction in various pathologic conditions and stabilize vulnerable plaques via suppression of inflammation [28]. More recently, Node et al. [23] reported that HMG-CoA reductase inhibitors improve cardiac function in patients with heart failure. The potent cardioprotective effects suggest that the pleiotropic effects of HMG-CoA reductase inhibitors are related to urocortin.

In the present study, we investigated whether urocortin is expressed in human endothelial cells. We also investigated the vascular action of urocortin and what factors regulate the expression of endothelial urocortin. Furthermore, the interaction of urocortin and HMG-CoA reductase inhibitor was investigated.

Methods

Cell Culture

HUVECs were obtained from Sanko Junyaku (Japan) and cultured in Medium 199 with 20% fetal bovine serum (FBS), 100 IU/ml heparin (Sigma Chemical Co., St. Louis, Mo., USA), 100 IU/ml endothelial cell growth supplement (BD Biosciences, Franklin Lakes, N.J., USA), 100 U/ml penicillin, and 100 μg/ml streptomycin. Cells were used between passages 4 and 8. Cells were stimulated with tumor necrosis factor-α (TNF-α), interferon-γ (IFN-γ), or pitavastatin at various concentrations for the indicated hours (0, 3, 6, and 24 h) in the presence of 5% FBS. Human recombinant TNF-α and IFN-γ were purchased from R&D Systems, Inc. (Mckinley Place NE, Minn., USA) and Diaclone Research (France), respectively. Pitavastatin was obtained from Kowa Pharmaceutical Company (Tokyo, Japan). After stimulation, the culture medium was collected for enzyme-linked immunosorbent assay (ELISA), and the cells were used for RNA isolation.

Measurement of Urocortin by ELISA

Serum urocortin and supernatants of cell culture medium were assayed by ELISA (Phoenix Pharmaceuticals Inc., Belmont, Calif., USA) according to the manufacturer's instructions. Assays were performed in polystyrene 96-well plates. The urocortin concentration was quantified against a standard curve calibrated with known amounts of protein. The upper detection limit for urocortin was 100 ng/ml. Each value is the mean of duplicate measurements.

Human Blood Sample and Study Design

Fifteen male volunteers, 25–41 years old, were included in the study. Participants were examined to exclude any pathologic disorders, which was confirmed with blood tests. Three volunteers were excluded because of mildly elevated levels of creatine phosphokinase or C-reactive protein (CRP). The remaining healthy subjects were treated with pitavastatin (2 mg/day) for 4 weeks. Blood samples were collected before and after pitavastatin treatment, and serum levels of lipids, CRP, and urocortin were measured. There were no reported adverse effects of pitavastatin. Written informed consent was obtained from all participants.

Immunohistochemistry

Immunohistochemistry for urocortin was performed on serial cryostat sections cut at 6 μm from frozen human coronary artery and heart muscle specimens. The sections were blocked with carrier protein for 30 min at room temperature, and then incubated with a primary antibody (rabbit anti-urocortin, IgG fraction of antiserum, Sigma Chemical Co.) (diluted 1:200) overnight at 4°C. The final concentration of primary antibody was 40 μg/ml. The sections were washed with phosphate-buffered saline (PBS), incubated with biotinylated goat anti-rabbit immunoglobulins (Dako) (diluted 1:500), washed in PBS, and finally incubated with streptavidin horseradish peroxidase conjugate (Dako LSAB kit™, Dako). For negative controls, the primary antibody was replaced with rabbit nonspecific immunoglobulin.

Reverse Transcription PCR and Measurement of Urocortin RNA Level

Total RNA was isolated from cultured HUVECs using a total RNA isolation kit (Isogen; Nippon Gene, Japan) according to the manufacturer's instructions. Complementary DNA was prepared using an RT-PCR kit (RETROscript™; Ambion). PCR were performed with *Taq* polymerase using the following specific primers. The primer sequences were as follows: human urocortin sense primer 5′-CAGGCGAGCGGCCGCG-3′, human urocortin antisense primer 5′-CTTGCCCACCGAGTCGAAT-3′. Urocortin cDNA amplification was performed in 40 cycles: samples were heated to 94°C for 1 min, cooled to 60°C for 1 min, and then heat-

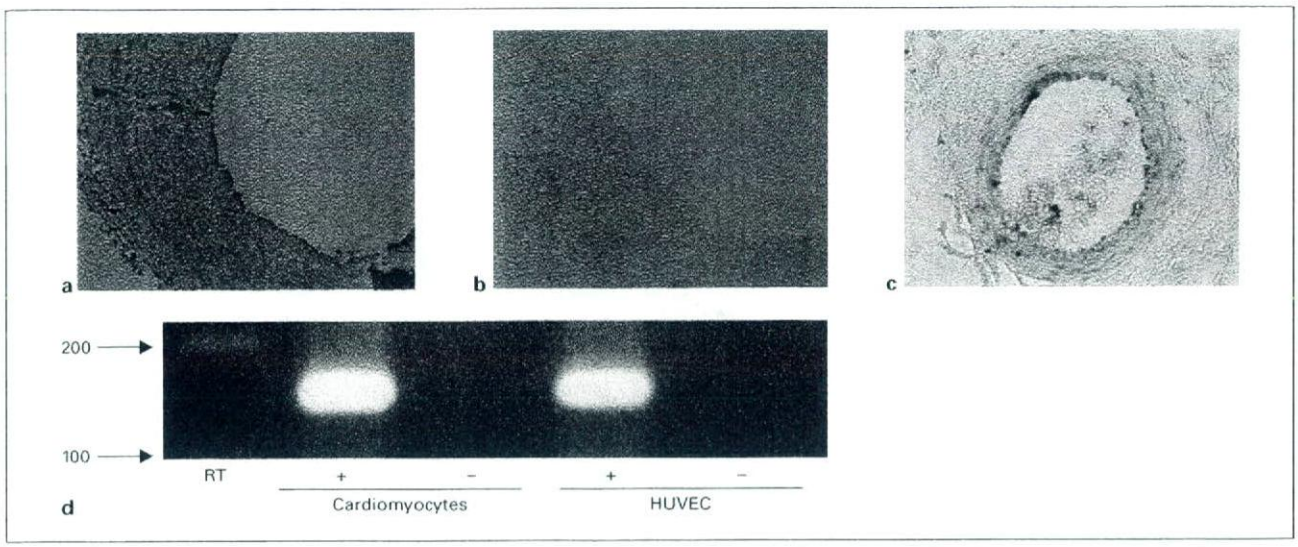

Fig. 1. Expression of urocortin in human endothelial cells. **a**, **c** Immunohistochemical analysis using epicardial coronary arteries (**a**) and microvessels in heart muscle (**c**) obtained from autopsy cases demonstrated positive urocortin immunoreactivity. **b** There was no significant staining when nonimmune serum was used as a control. **d** RT-PCR confirmed the expression of urocortin in cultured HUVECs. Human cardiomyocytes were used as a positive control.

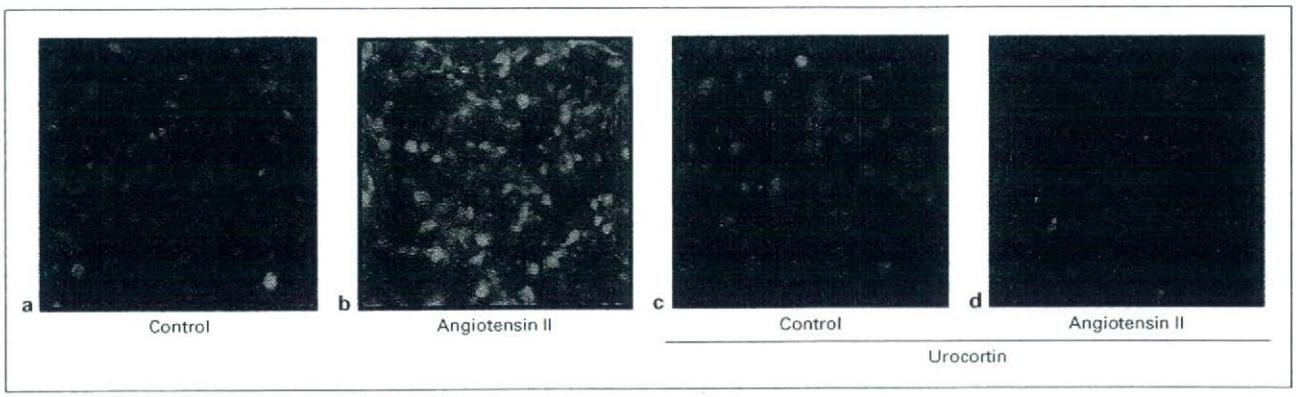

Fig. 2. Effects of urocortin on intracellular ROS in HUVECs assessed by the H_2DCFDA method. **a**, **b** Incubation with angiotensin II (10^{-7} *M*) induced the generation of intracellular ROS in HUVECs. **c**, **d** Coincubation with urocortin (10^{-8} *M*) significantly suppressed angiotensin II-induced intracellular ROS generation.

ed at 72°C for 1 min. PCR products were separated using 2% agarose gels stained with ethidium bromide and visualized under UV light. PCR products were purified and further analyzed by DNA sequencing using an ABI Prism BigDye Terminator Cycle Sequencing kit on an ABI Prism 310 Genetic Analyzer. To measure the production of urocortin mRNA, RT-PCR for GAPDH was also performed (sense primer 5′-ACGGATTTGGTCGTATTGGGC-3′, antisense primer 5′-TTGACGGTGCCATGGAATTTG-3′). Photographs of the ethidium-bromide-stained gels were scanned, and band intensities were measured using a densitometer (ATTO Lane Analyzer 3.0; ATTO Co., Tokyo, Japan). The quantity of the urocortin mRNA was determined by the ratio of urocortin and GAPDH band intensities.

Evaluation of Intracellular ROS in HUVECs

Intracellular ROS were detected with 2′,7-dichlorodihydrofluoresceindiacetate (H_2DCFDA, Molecular Probes, Eugene, Oreg., USA). As described before [31], a confluent monolayer of HUVECs was treated with angiotensin II (10^{-7} *M*) (Sigma Chemical Co.) or human urocortin (10^{-8} *M*) (Phoenix Pharmaceuticals Inc.) for 1 h,

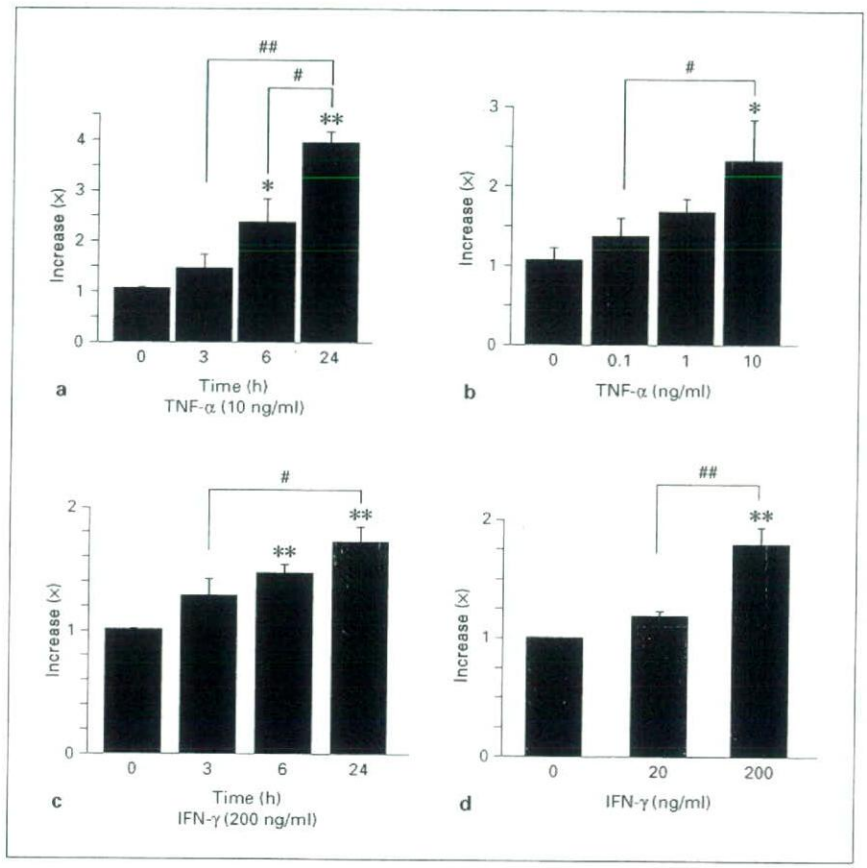

Fig. 3. Effects of TNF-α (**a**, **b**) or IFN-γ (**c**, **d**) on the release of urocortin from HUVECs. **a**, **b** HUVECs were incubated with TNF-α (10 ng/ml) for the indicated time periods (**a**) or for 6 h with the indicated concentration of TNF-α (**b**). **c**, **d** HUVECs were incubated with IFN-γ (200 ng/ml) for the indicated time periods (**c**) or for 6 h with the indicated concentration of IFN-γ (**d**). After stimulation, the concentration of urocortin in the conditioned medium was assessed by ELISA. Data were plotted as mean ± SEM from three independent experiments performed in duplicate. * $p < 0.05$; ** $p < 0.01$ vs. control; # $p < 0.05$; ## $p < 0.01$.

then they were treated with H_2DCFDA (10 μM) for 30 min at 37°C in the dark. The fluorescence intensity was measured using a laser-scanning confocal imaging system.

Statistical Analysis

Data are presented as mean ± SEM. Statistical analysis was performed by analysis of variance followed by Fisher's PLSD test. $p < 0.05$ was considered to be statistically significant.

Results

Human Endothelial Cells Express Urocortin

First, we examined whether human endothelial cells express urocortin. As shown in figure 1, immunohistochemical analysis using specimens obtained from autopsy cases demonstrated positive immunoreactivity of urocortin in human epicardial coronary artery endothelial cells (fig. 1a) and endothelial cells of microvessels in heart muscle (fig. 1c), whereas there was no signal when non-immune serum was used (fig. 1b). Preabsorbance of the primary antibody with 10^{-8}–10^{-6} M of urocortin significantly suppressed the immunoreactivity. Next, to confirm its expression in endothelial cells, RT-PCR was performed using sets of urocortin-specific primers. Urocortin mRNA was detected by RT-PCR in HUVECs (fig. 1d). No RT-PCR product was present in the negative control in which RT was not performed. Sequencing of complementary DNA of urocortin obtained from HUVECs was the same as the sequence obtained from neurons (data not shown). Thus, urocortin is expressed in human endothelial cells.

Urocortin Suppressed ROS Generation in HUVECs

We investigated the effects of urocortin on ROS generation of HUVECs by H_2DCFDA. Incubation with angiotensin II (10^{-7} M) induced the generation of ROS in HUVECs (fig. 2). Urocortin (10^{-8} M) significantly suppressed angiotensin II-induced ROS generation.

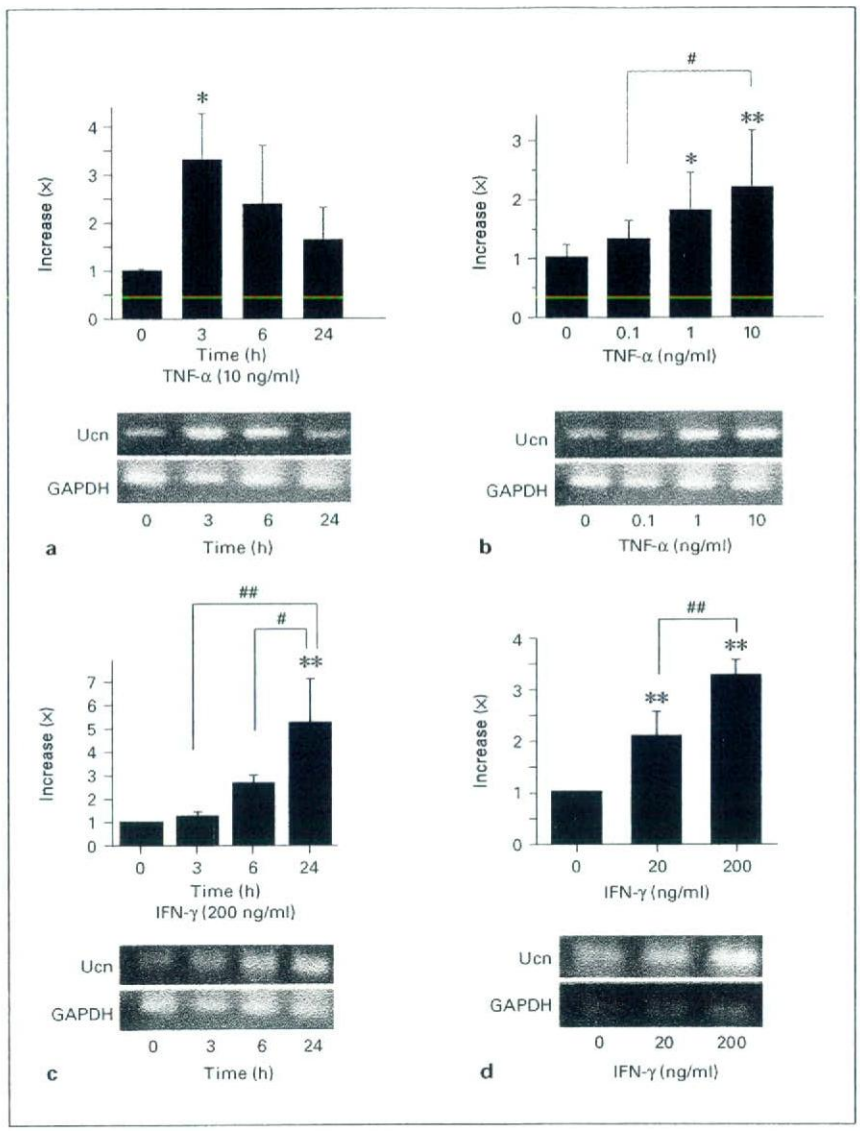

Fig. 4. Effects of TNF-α (**a**, **b**) or IFN-γ (**c**, **d**) on urocortin (Ucn) mRNA in HUVECs assessed by RT-PCR. **a**, **b** HUVECs were incubated with TNF-α (10 ng/ml) for the indicated time periods (**a**) or for 6 h with the indicated concentration of TNF-α (**b**). **c**, **d** HUVECs were incubated with IFN-γ (200 ng/ml) for the indicated time periods (**c**) or for 6 h with the indicated concentration of IFN-γ (**d**). After stimulation, mRNA levels of urocortin were assessed by RT-PCR. Densitometric analysis of five independent experiments. * $p < 0.05$; ** $p < 0.01$ vs. control; # $p < 0.05$; ## $p < 0.01$.

Expression of Endothelial Urocortin Was Increased by Inflammatory Cytokines and Pitavastatin

Because previous studies demonstrated that various cytokines modulate the expression of urocortin in neurons, the effects of inflammatory cytokines on expression of endothelial urocortin were examined by ELISA. Incubation with TNF-α (10 ng/ml) resulted in increased urocortin production in a time- and dose-dependent manner (fig. 3a, b). IFN-γ also increased the urocortin release from HUVECs (fig. 3c, d).

RT-PCR demonstrated that TNF-α and IFN-γ increased the steady state urocortin mRNA levels in HUVECs (fig. 4). Incubation with pitavastatin (0.1–3.0 μ*M*) potently increased the release of urocortin from HUVECs in a dose-dependent manner (fig. 5a). RT-PCR revealed modestly increased urocortin mRNA from HUVECs (fig. 5b).

Treatment with Pitavastatin Increases Serum Urocortin Levels in Humans

The findings using cultured HUVECs prompted us to examine the effects of treatment with pitavastatin on plasma urocortin levels in humans. Treatment with pitavastatin (2 mg/day) for 4 weeks decreased total cho-

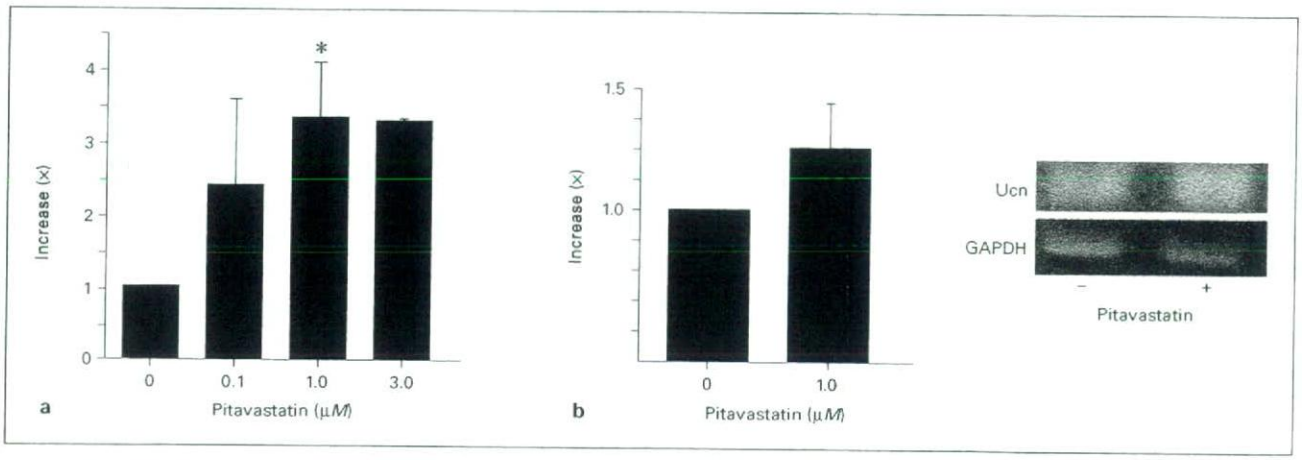

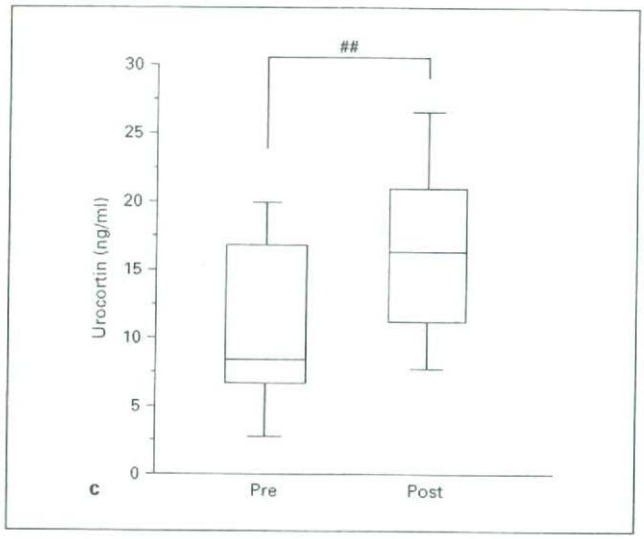

Fig. 5. a, **b** Effects of pitavastatin on urocortin release (**a**) and its mRNA (**b**) in HUVECs. HUVECs were incubated with pitavastatin with the indicated concentration for 24 h. After stimulation, the concentration of urocortin in the conditioned medium was assessed by ELISA (**a**). Data were plotted as mean ± SEM from three independent experiments, performed in duplicate. Pitavastatin-induced changes in urocortin mRNA were assessed by RT-PCR (**b**). Densitometric analysis of three independent experiments. * $p < 0.05$ vs. control. **c** Treatment with pitavastatin increases serum levels of urocortin in humans. Treatment with pitavastatin (2 mg/day) for 4 weeks increased urocortin levels in healthy male volunteers. ## $p < 0.01$.

Table 1. Change of serum levels of various parameters by pitavastatin

Charasteristics	Mean ± SD (pre)	Mean ± SD (post)
Blood glucose	96 ± 10.4	93 ± 6.5
Total cholesterol, mg/dl	192.8 ± 29.7	149.2 ± 27.4***
TG, mg/dl	88.4 ± 44.6	86.4 ± 40.3
HDL cholesterol, mg/dl	69.6 ± 15.1	67 ± 15.3
LDL cholesterol, mg/dl	100.0 ± 25.4	61.0 ± 22.5***
hsCRP, ng/ml	257.5 ± 235.9	254.1 ± 248.6
Serum urocortin, ng/ml	11.0 ± 6.5	16.4 ± 7.3**

Treatment with pitavastatin (2 mg/day) for 4 weeks significantly decreased total cholesterol and LDL cholesterol levels. Pitavastatin significantly increased serum urocortin levels. *** $p < 0.0001$ vs. pre. ** $p < 0.01$ vs. pre.

lesterol and LDL levels (table 1). Interestingly, pitavastatin increased urocortin levels from 11.0 ± 6.5 to 16.4 ± 7.3 ng/ml in healthy male volunteers (fig. 5c).

Discussion

Urocortin was originally identified in the central nervous system [1–3]; however, there is considerable evidence indicating that urocortin is also expressed in other organs, including the gastrointestinal [5], immune [6, 7] and cardiovascular systems [9]. There is no direct evidence, however, that urocortin is expressed in the vasculature. The present investigation is the first study to demonstrate that urocortin is expressed in endothelial cells.

Furthermore, urocortin (10^{-8} *M*) potently suppressed ROS generation induced by angiotensin II in HUVECs. TNF-α and IFN-γ increased urocortin mRNA level and its release from HUVECs. Interestingly, incubation with pitavastatin significantly increased urocortin mRNA levels and its release from HUVECs. Thus, endothelial urocortin is upregulated by inflammatory cytokines and pitavastatin, and it has anti-oxidative properties in endothelial cells. Furthermore, treatment with pitavastatin for 4 weeks increased the serum urocortin levels in healthy male volunteers.

Urocortin is expressed in various immunocompetent cells such as macrophages and lymphocytes [7], and in inflammatory lesions. For example, Kohno et al. [6] reported that urocortin is expressed in the synovium of rheumatoid arthritis patients. The expression of immunoreactive urocortin in rheumatoid arthritis patients correlates with the extent of inflammatory infiltrates [6]. On the other hand, the concentration of immunoreactive urocortin was higher in gastric biopsies obtained from patients with active *Helicobacter pylori* gastritis than in normal controls [5]. After the apparent eradication of *H. pylori* infection, immunoreactive urocortin levels increased dramatically compared with pretreatment values. These findings strongly suggest that urocortin has a possible role in the pathogenesis of these inflammatory diseases. There remains controversy, however, as to whether urocortin exerts proinflammatory or anti-inflammatory effects. Urocortin increases the secretion of interleukin-6 from peripheral blood mononuclear cells [6], suggesting it has proinflammatory actions. In contrast, Agnello et al. [24] reported that urocortin significantly reduces lipopolysaccharide-induced serum TNF-α and interleukin-1β levels in mice. In the present investigation, urocortin potently suppressed ROS generation in HUVECs, whereas inflammatory cytokines increased urocortin expression and its release from HUVECs. Taken together, these findings suggest that endothelial urocortin acts as an anti-oxidative factor, and the upregulation of urocortin by inflammatory cytokines is part of a counter-regulatory mechanism against oxidative stress in inflammatory lesions.

Recently, a wide variety of pleiotropic effects of HMG-CoA reductase inhibitors was proposed, including improvement of endothelial function, stabilization of vulnerable plaque, anti-coagulation effects, anti-inflammatory effects, anti-oxidative effects, etc. [29, 30]. Treatment with HMG-CoA reductase inhibitors improves the functional classification of the New York Heart Association and left ventricular ejection fraction in patients with dilated cardiomyopathy [23]. Furthermore, plasma concentrations of TNF-α, interleukin-6, and brain natriuretic peptide are also significantly decreased by HMG-CoA reductase inhibitor treatment [23]. Thus, HMG-CoA reductase inhibitors likely induce potent cardioprotective effects. In the present study, pitavastatin increased the release of urocortin from HUVECs. There was no statistically significant increase in urocortin mRNA levels after incubation with pitavastatin, although mRNA levels tended to increase. Posttranscriptional regulation may mediate the increase in urocortin mRNA levels during incubation with pitavastatin. Furthermore, treatment with pitavastatin increased the serum urocortin levels in humans. Given its potent cardioprotective effects, urocortin might be partly involved in the mechanisms of the pleiotropic effects of HMG-CoA reductase inhibitors in the vasculature. The pitavastatin-induced increase in urocortin may originate from several possible sources, including the central and peripheral nervous systems, cardiomyocytes, and endothelial cells. Further investigation is needed to clarify the precise mechanisms whereby pitavastatin increases the serum urocortin levels.

In conclusion, urocortin was expressed in human endothelial cells. Endothelial urocotin is upregulated by inflammatory cytokines and pitavastatin, and it suppressed the production of ROS in endothelial cells. Treatment with pitavastatin increased the serum urocortin levels in human subjects. Endothelial urocortin might exert anti-oxidative effects in inflammatory lesions and this might partially explain the mechanisms of various pleiotropic effects of statins.

References

1 Vaughan J, Donaldson C, Bittencourt J, Perrin MH, Lewis K, Sutton S, Chan R, Turnbull AV, Lovejoy D, River C: Urocortin, a mammalian neuropeptide related to fish urotensin 1 and to corticotrophin-releasing factor. Nature 1995; 378:287–292.

2 Iino K, Sasano H, Oki Y, Andoh N, Shin RW, Kitamoto T, Totsune K, Suzuki H, Nagura H, Yoshimi T: Urocortin expression in human pituitary gland and pituitary adenoma. J Clin Endocrinol Metab 1997;82:3842–3850.

3 Takahashi K, Totsune K, Sone M, Murakami O, Satoh F, Arihara Z, Sasano H, Iino K, Mouri T: Regional distribution of urocortin-like immunoreactivity and expression of urocortin mRNA in the human brain. Peptide 1998;19: 643–647.

4 Petraglia F, Florio P, Gallo R, Simoncini T, Saviozzi M, Di Blasio AM, Vaughan J, Vale W: Human placenta and fetal membranes express human urocortin mRNA and peptide. J Clin Endocrinol Metab 1996;81:3807–3810.

5 Chatzaki E, Charalampopolos I, Leontidis C, Mouzas IA, Tzardi M, Tsatsanis C, Margioris AN, Gravanis A: Urocortin in human gastric mucosa: relationship to inflammatory activity. J Clin Endocrinol Metab 2003;88:478–483.

6 Kohno M, Kawahito Y, Tsubouchi Y, Hashiramoto A, Yamada R, Inoue K, Kusaka Y, Kubo T, Elenkov IJ, Chrousos G, Kondo M, Sano H: Urocortin expression in synovium of patients with rheumatoid arthritis and osteoarthritis: relation to inflammatory activity. J Clin Endocrinol Metab 2001;86:4344–4352.

7 Bamberger CM, Wald M, Bamberger AM, Ergun S, Beri FU, Schulte HM: Human lymphocytes produce urocortin, but not corticotropin-releasing hormone. J Clin Endocrinol Metab 1998;83:708–711.

8 Seres J, Bornstein SR, Seres P, Willenberg HS, Schulte KM, Scherbaum WA, Ehrhart-Bornstein M: Corticotropin-releasing hormone system in human adipose tissue. J Clin Endocrinol Metab 2004;89:965–970.

9 Kimura Y, Takahashi K, Totsune K, Muramatsu Y, Kaneko C, Darnel AD, Suzuki T, Ebina M, Nukiwa T, Sasano H: Expression of urocortin and corticotrophin-releasing factor receptor subtypes in the human heart. J Clin Endocrinol Metab 2002;87:340–346.

10 Rademaker MT, Charles CJ, Espiner E, Fisher S, Frampton CM, Kirkpatrick CMJ, Lainchbury J, Nicholls G, Richards M, Vale W: Beneficial hemodynamic, endocrine, and renal effects of urocortin in experimental heart failure: comparison with normal sheep. J Am Coll Cardiol 2002;40:1495–1505.

11 Huag Y, Chan F, Lau CW, Tsang SY, Chen ZY, He GW, Yao X: Roles of cyclic AMP and Ca^{2+}-activated K^+ channels in endothelium-independent relaxation by urocortin in the rat coronary artery. Cardiovascular Research 2003;57:824–833.

12 Parkes DG, Vaughan J, Rivier J, Vale W, May CN: Cardiac inotropic actions of urocortin in conscious sheep. Am J Physiol 1997;272: H2115–H2122.

13 Scarabelli TM, Pasini E, Stephanou A, Comini L, Curello S, Raddino R, Ferrari R, Knight R, Latchman D: Urocortin promotes hemodynamic and bioenergic recovery and improves cell survival in the isolated rat heart exposed to ischemia/reperfusion. J Am Coll Cardiol 2002;40:155–161.

14 Gordon JM, Gregory JD, Owen LW, Dusting GJ, Woodman OL: Cardioprotective action of CRF peptide urocortin against stimulated ischemia in adult rat cardiomyocytes. Am J Physiol Heart Circ Physiol 2003;284:H330–H336.

15 Lawrence KM, Chanalaris A, Scarabelli T, Hubank M, Pasini E, Townsend PA, Comini L, Ferrari R, Tinker A, Stephanou A, Kight R, Litchman D: K_{ATP} channel gene expression is induced by urocortin and mediates its cardioprotective effect. Circulation 2002;106:1556–1562.

16 Schulman D, Latchman DS, Yellon DM: Urocortin protects the heart from reperfusion injury via upregulation of p42/p44 MAPK signaling pathway. Am J Physiol Heart Circ Physiol 2002;283:H1481–H1488.

17 Brar BK, Jonassen AK, Stephanou A, Santilli G, Railson J, Knight RA, Yellon DM, Latchman DS: Urocortin protects against ischemic and reperfusion injury via a MAPK-dependent pathway. J Biol Chem 2000;275:8508–8514.

18 Kishimoto T, Pearse RV, Lin CR, Rosenfeld MG: A sauvagine/corticotrophin-releasing factor receptor expressed in heart and skeletal muscle. Proc Natl Acad Sci USA 1995;92: 1108–1112.

19 Wiley KE, Davenport AP: CRF2 receptors are highly expressed in the human cardiovascular system and their cognate ligands urocortins 2 and 3 are potent vasodilators. Br J Pharmacol 2004;143:508–514.

20 Coste SC, Kesterson RA, Heldwein KA, Stevens SL, Heard AD, Hollis JH, Murray SE, Hill JK, Pantely GA, Hohimer AR, Hatton DC, Phillips TJ, Finn DA, Low MJ, Rittenberg MB, Stenzel P, Stenzel-Poore MP: Abnormal adaptations to stress and impaired cardiovascular function in mice lacking corticotropin-releasing hormone receptor-2. Nat Genet 2000;24: 403–409.

21 Florio P, Arcuri F, Ciarmela P, Runci Y, Romagnoli R, Cintorino M, Di Blasio AM, Petraglia F: Identification of urocortin mRNA and peptide in the human endometrium. J Endocrinol 2002;173:R9–R14.

22 Simoncini T, Apa R, Reis FM, Miceli F, Stomati M, Driul L, Lanzone A, Genazzani AR, Petraglia F: Human umbilical vein endothelial cells: a new source and potential target for corticotropin-releasing factor. J Clin Endocrinol Metab 1999;84:2802–2806.

23 Node K, Fujita M, Kitakaze M, Hori M, Liao JK: Short-term statin therapy improves cardiac function and symptom in patients with idiopathic dilated cardiomyopathy. Circulation 2003;108:839–843.

24 Agnello D, Bertini R, Sacco S, Meazza C, Villa P, Ghezzi P: Corticosteroid-independent inhibition of tumor necrosis factor production by the neuropeptide urocortin. Am J Physiol 1998;275:E757–E762.

25 Ridker PM, Rifai N, Pfeffer MA, Sacks F, Braunwald E: Long-term effects of pravastatin on plasma concentration of C-reactive protein. Circulation 1999;100:230–235.

26 Ridker PM, Rifai N, Lowenthal SP: Rapid reduction in C-reactive protein with cerivastatin among 785 patients with primary hypercholesterolemia. Circulation 2001;103:1191–1193.

27 Rikitake Y, Kawashima S, Takeshita S, Yamashita T, Azumi H, Yasuhara M, Nishi H, Inoue N, Yokoyama M: Anti-oxidative properties of fluvastatin, an HMG-CoA reductase inhibitor, contribute to prevention of atherosclerosis in cholesterol-fed rabbits. Atherosclerosis 2001;154:87–96.

28 Treasure CB, Klein L, Weintraub WS, Talley JD, Stillabower ME, Kosinski AS, Zhang J, Boccuzzi S, Cedarholm J, Alexander W: Beneficial effects of cholesterol-lowering therapy on the coronary endothelium in patients with coronary artery disease. N Engl J Med 1995; 332:481–487.

29 Takamoto M, Liao JK: Pleiotropic effects of 3-hydoxy-3-methylglutaryl coenzyme A reductase inhibitors. Arterioscler Tromb Vasc Biol 2001;21:1712–1719.

30 Liao JK: Beyond lipid lowering: the role of statins in vascular protection. Int J Cardiol 2002;86:5–18.

31 Kobayashi S, Inoue N, Ohashi Y, Terashima M, Matsui K, Mori T, Fujita H, Awano K, Kobayashi K, Azumi H, Ejiri J, Hirata K, Kawashima S, Hayashi Y, Yokozaki H, Itoh H, Yokoyama M: Interaction of oxidative stress and inflammatory response in coronary plaque instability: important role of C-reactive protein. Arterioscler Thromb Vasc Biol 2003;23: 1398–1404.

ELSEVIER

Atherosclerosis 186 (2006) 402–410

ATHEROSCLEROSIS

www.elsevier.com/locate/atherosclerosis

Angiotensin II type 1 receptor blocker telmisartan suppresses superoxide production and reduces atherosclerotic lesion formation in apolipoprotein E-deficient mice

Tomofumi Takaya, Seinosuke Kawashima*, Masakazu Shinohara, Tomoya Yamashita, Ryuji Toh, Naoto Sasaki, Nobutaka Inoue, Ken-ichi Hirata, Mitsuhiro Yokoyama

Division of Cardiovascular and Respiratory Medicine, Department of Internal Medicine, Kobe University Graduate School of Medicine, 7-5-2, Kusunoki-cho, Chuo-ku, Kobe 650-0017, Japan

Received 28 December 2004; received in revised form 3 June 2005; accepted 1 August 2005
Available online 12 September 2005

Abstract

Angiotensin II is involved in the process of atherosclerosis and stimulates superoxide production from cardiovascular cells. We examined the effect of telmisartan, an angiotensin II type 1 receptor blocker, on atherosclerosis. We chronically treated apolipoprotein E-deficient mice with two different doses of telmisartan dissolved in drinking water (0.3 and 3 mg/kg) starting from 4 weeks of age for 12 weeks. Lipid contents were not different in both telmisartan-treated groups compared with control group. Systolic blood pressure was significantly reduced with 3 mg/kg, but unchanged with 0.3 mg/kg. The total atherosclerotic lesion size at the aortic sinus was reduced with 0.3 mg/kg compared with control, and additional reduction was proved with 3 mg/kg. The fibrotic change was not different among three groups, but MOMA-2-, malondialdehyde-, 4-hydroxy-2-nonenal-immunostained areas were reduced by telmisartan. As the mechanism, we revealed that both doses of telmisartan markedly reduced superoxide production from in situ vessels assessed by lucigenin-enhanced chemiluminescence and dihydroethidium staining. And NAD(P)H dependent oxidase activity in vessels was reduced by telmisartan. Further, 8-*iso*-prostaglandin F2α level, a systemic oxidative stress marker, obtained from urine and plasma samples were significantly reduced by telmisartan. Telmisartan reduced atherosclerosis in apolipoprotein E-deficient mice at least partly via the suppression of oxidative stress.

Keywords: Angiotensin II type 1 receptor blocker; Atherosclerosis; Oxidative stress; Apolipoprotein E-deficient mouse

1. Introduction

The renin-angiotensin system (RAS) plays important roles in the regulation of not only blood pressure but also vascular structure. The main component of RAS is angiotensin II (Ang II), which is a potent vasoconstrictor and elevates blood pressure. Ang II generates aldosterone and activates sympathetic nervous system, leading to blood pressure elevation.

Besides its effect on blood pressure, a number of evidence revealed that Ang II is involved in atherogenesis. In animal models, chronic infusion of Ang II promotes atherosclerotic lesion formation [1]. It is shown that Ang II promotes atherogenesis via direct effects on vascular beds independent of hypertensive effects. Among them, the effect as the inducer of oxidative stress is recently attracting attention. In atherosclerosis, there is augmented production of reactive oxygen species (ROS) from various cell types including endothelial cells, vascular smooth muscle cells and monocytes/macrophages, and Ang II plays a pivotal role in their production [2–4]. There are increased expressions of angiotensin converting enzyme (ACE) and Ang II type 1 receptor in atherosclerotic arteries, indicating the presence of augmented local RAS activation [5,6]. Ang II increases superoxide production from vessel wall by activating NAD(P)H oxidase [7]. ROS are closely implicated

* Corresponding author. Tel.: +81 78 382 5845; fax: +81 78 382 5859.
E-mail address: kawashim@med.kobe-u.ac.jp (S. Kawashima).

0021-9150/$ – see front matter © 2005 Elsevier Ireland Ltd. All rights reserved.
doi:10.1016/j.atherosclerosis.2005.08.009

in atherogenesis, by damaging and activating the endothelium, oxidizing low-density lipoprotein (LDL) cholesterol, and promoting proliferation of vascular smooth muscle cells. They also induce various genes such as those of adhesion molecules and chemokines, which play important roles in the initiation and progression of atherosclerotic lesion formation [8,9].

ACE inhibitors (ACE-I) and Ang II type 1 receptor blockers (ARB) are widely used for treatment of hypertension to prevent organ damages. These drugs have been already reported to prevent atherosclerosis in several studies using animal models [10–13]. Losartan reduced atherosclerotic lesion formation without changing blood pressure in cynomologous monkeys [10] and apolipoprotein E-deficient (apoE-KO) mice [11]. Olmesartan was reported to reduce atherosclerosis in association with suppressions of serum macrophage-colony stimulating factor, transforming growth factor-beta 1 and intracellular adhesion molecule-1 in monkeys fed a high cholesterol chow [13].

There has been little information whether ARB can show anti-atherogenic effects by the mechanisms related to suppression of oxidative stress. In the present study, we investigated the effects of telmisartan, an ARB, on atherosclerotic lesion formation in apoE-KO mice. Particularly, we examined whether the effects of telmisartan on atherogenesis were independent of its effect on blood pressure and associated with changes in oxidative stress.

2. Materials and methods

2.1. Materials and animal preparation

Telmisartan was obtained from Boehringer Ingelheim Inc. (Germany). All other commercial drugs used in this study were purchased from Sigma Chemical Co. (MO). ApoE-KO mice on a C57BL/6 genetic background at 4 weeks of age were assigned to control group and two telmisartan-treatment groups given different dosages. Drug treatment consisted of 0.3 and 3 mg/kg body weight per day of telmisartan dissolved in drinking water. Mice were fed a standard chow and supplemented with telmisartan for next 12 weeks and sacrificed at 16 weeks of age. Animals were provided the chow and water ad libitium and maintained on a 12 h light/dark cycle. All animal experiments were conducted according to the guidelines for animal experiments at Kobe University Graduate School of Medicine.

2.2. Plasma analysis

After overnight fasting, blood was collected by the cardiac puncture into heparin-coated tubes under anesthetic condition using pentobarbital sodium (80 mg/kg intraperitoneal injection). Plasma was obtained through centrifugation of the blood for 10 min at 5500 × *g* at 4 °C and stored at −80 °C until each assay. Concentrations of plasma total cholesterol and triglyceride were determined by use of an automated clinical chemistry analyzer. High-density lipoprotein cholesterol levels were quantified by enzymatic reaction using a commercially available kit (Wako, Japan). Glucose levels were determined by glucometer (Sanwa Kagaku, Japan) and insulin levels were determined with a commercially available kit (LINCO Research Inc., MO).

2.3. Hemodynamic analysis

Heart rate and systolic blood pressure of apoE-KO mice were measured at 16 weeks of age using the tail-cuff method without heating. The mouse tail was placed into a device with a rubber cuff and a photoelectric sensor, and heart rate and systolic blood pressure were measured using MK-2000 (Muromachi Kikai, Japan). All measurements were repeated six times for each mouse.

2.4. Atherosclerotic lesion assessment at the aortic sinus

After 12 weeks of telmisartan treatment, both gender mice (16 weeks of age) were anesthetized as above and the aorta was perfused with normal saline containing 10 U/ml heparin. Then the aorta sample was dissected from the middle of the left ventricle to the aortic arch, and fixed with 4% paraformaldehyde for overnight. The sample was cut in the ascending aorta, and the proximal sample containing the aortic sinus was embedded in OCT compounds (Tissue-Tek, CA). Five consecutive sections (10 μm thickness), spanning 550 μm of the aortic sinus, were collected from each mouse and stained with Sudan III and Masson's trichrome. For quantitative analysis of atherosclerosis, the average lesion area of five separate sections from each mouse was obtained with the use of the Image J (National Institutes of Health, MD) according to the method described by Paigen et al. [14].

2.5. Immunohistochemistry

Immunohistochemical staining with MOMA-2 (BMA Biomedicals AG, Switzerland; 1:500 dilution), malondialdehyde (MDA) (Alpha Diagnostic International Inc., TX; 1:100 dilution) and 4-hydroxy-2-nonenal (HNE) (Alpha Diagnostic International Inc., TX; 1:100 dilution) of atherosclerotic lesions at the aortic sinus was performed by the labeled streptaviadin biotin method as previously reported [15]. Quantitative analysis of MOMA-2-immunostaining was evaluated as a ratio of the positive-stained area to total plaque area in the atherosclerotic lesion at the aortic sinus.

2.6. Measurement of superoxide production from aortas

After euthanization of mice, the aorta was cut out from the aortic arch to the bifurcation of iliac arteries and the tissues around the vessel were cleaned. Then the aorta were cut into four pieces (approximately 5 mm length per each pieces) and

these aortic rings were incubated with the Cu–Zn superoxide dismutase inhibitor for 30 min at 37 °C, and vascular superoxide production levels were measured by chemiluminescence (CL) with 10 μM lucigenin (bis-*N*-methylacridinium nitrate). The final volume of lucigenin solution was 1 mL. The light reaction between superoxide and lucigenin was detected with a BLR-201 CL reader (ALOKA, Japan) and photon emission was continuously recorded for 15 min. The CL signal was expressed as the average count per minute (C.P.M.) for 15 min periods and the counts were corrected by vessel dry weights.

2.7. Measurement of NAD(P)H dependent oxidase activity of aorta homogenates

The aorta was cut out from each mouse as described above, and the aortic segments (almost 2 cm length) were placed in a chilled modified 50 mM HEPES/PSS buffer and homogenized on ice with a motor-driven tissue homogenizerfor 1 min in 200 μL homogenate buffer, which contained 0.01 mM EDTA. The homogenates were centrifuged at 1000 × *g* for 10 min. The pellet was discarded and the supernatant was stored on ice until use. Protein concentration of aorta homogenate was measured by the method of Bradford [16]. The assay solution contained 50 mM HEPES/PSS (pH 7.4), 1 mM EDTA, 6.5 mM $MgCl_2$, 83 mM sucrose, and 250 μM lucigenin as the electron acceptor and 100 μM NADH or 100 μM NADPH as the electron donor [17]. After pre-incubation at 37 °C for 20 min, the reaction was started by adding 20 μL of aorta homogenates. All CL data were evaluated after subtracting the CL counts obtained in the absence of homogenates. Each count was corrected by protein levels of aorta homogenate.

In some experiments, we examined the effects of 100 μM diphenylene iodonium (DPI), an inhibitor of all flavoenzymes, and 500 μM apocynin, an inhibitor of NAD(P)H oxidase, on superoxide production after stimulation of homogenates with NAD(P)H. The aorta homogenates were pre-incubated with each agent for 15 min before CL measurement.

2.8. In situ detection of superoxide production in aortas and endothelial cells

To evaluate in situ superoxide production from vessels, unfixed frozen cross sections of aortas were stained with dihydroethidium (DHE; Molecular Probe, OR) according to the previously validated method [18]. In the presence of superoxide, DHE is converted to the fluorescent molecule ethidium, which can then label nuclei by intercalating with DNA. Briefly, the unfixed frozen tissues were cut into 10 μm thick sections, and incubated with 10 μM DHE at 37 °C for 30 min in a light-protected humidified chamber. The images were obtained with a laser scanning confocal microscope (Carl ZEISS, Germany). Superoxide production was demonstrated by red fluorescence labeling.

For quantification of ethidium fluorescence from endothelial cells, fluorescence (intensity × area) was measured only on the luminal side of the internal elastic lamina using the Image J in high-power (100×) images [19]. For each vessel, total fluorescence was calculated from three separate high-power fields taken in each section of the vessel to produce $n = 1$.

2.9. Measurement of 8-iso-prostaglandin F2α and serum amyloid A levels

Urine samples were collected from mice at the age of 12–16 weeks, and stored at −80 °C after addition of butyrated hydroxytoluene (BHT) at a final concentration of 0.01%. After purification using C18 reverse phase extraction column (Waters Corporation, MA), urine 8-*iso*-prostaglandin (PG) F2α levels were measured with EIA kits (Assay Designs Inc., MI) according to the manufacturer's instructions, and data were corrected by urine creatinine levels. Plasma samples were collected as above and stored at −80 °C after addition of BHT at a final concentration of 0.01%. We measured direct 8-*iso*-PGF2α levels from plasma samples with EIA kits (Assay Designs Inc., MI) according to the manufacturer's instructions.

We collected plasma from each mouse as shown in Section 2 and measured serum amyloid A (SAA) levels with mouse SAA ELISA kit (BioSource International Inc., CA) according to the manufacturer's instructions.

2.10. Statistical analysis

Data were expressed as mean ± S.E.M. One-way ANOVA was used to compare the differences among three groups with Fisher's PLSD test for post hoc analysis. Values of $P < 0.05$ were considered statistically significant.

Table 1
Effect of telmisartan on body weight, lipid contents, glucose and insulin levels, and vital signs

	Control	0.3 mg/kg	3 mg/kg
Female body weight (g)	21.8 ± 0.5	21.2 ± 0.3	21.2 ± 0.5
Male body weight (g)	26.9 ± 0.6	27.0 ± 0.4	26.7 ± 1.5
Total cholesterol (mg/dl)	478.6 ± 28.8	463.4 ± 19.1	464.9 ± 22.8
Triglyceride (mg/dl)	53.5 ± 6.8	50.0 ± 9.7	57.8 ± 8.1
HDL cholesterol (mg/dl)	9.4 ± 0.8	9.3 ± 0.9	9.0 ± 0.7
Glucose (mg/dl)	108.4 ± 8.2	116.1 ± 7.1	112.5 ± 5.5
Insulin (ng/ml)	0.24 ± 0.12	0.18 ± 0.06	0.24 ± 0.05
Heart rate (min^{-1})	543.9 ± 50.8	536.3 ± 89.7	540.5 ± 76.7
Systolic BP (mmHg)	107.4 ± 1.7	106.9 ± 2.1	90.1 ± 1.8*

Mice were fed a standard chow for 16 weeks and body weight of each mouse was measured. Mice were fasted for at least 12 h and bled, and plasma total cholesterol, triglyceride, high-density lipoprotein cholesterol, glucose and insulin levels were determined as described in Section 2 ($n = 8$ per group). Heart rate and systolic blood pressure were measured with the use of the tail-cuff method ($n = 15$ per group). Results were expressed as mean ± S.E.M.; BP, blood pressure.

* $P < 0.0001$ vs. control.

3. Results

3.1. The effects of telmisartan on blood pressure and plasma lipid levels

Body weight was not significantly different among three groups of each gender (Table 1). Neither plasma total cholesterol, triglyceride, nor high-density lipoprotein cholesterol levels were affected by the treatment with telmisartan. And neither plasma glucose, nor insulin levels were affected by the treatment with telmisartan. Although heart rate was not affected, 3 mg/kg telmisartan significantly reduced systolic blood pressure compared with that of control group (Table 1). In contrast, 0.3 mg/kg telmisartan did not change systolic blood pressure.

3.2. Atherosclerotic lesion formation at the aortic sinus

After feeding a standard chow for 16 weeks, the atherosclerotic lesion formation was assessed at the aortic sinus. Representative photographs of each mouse were shown in Fig. 1A. In quantitative analysis of histological examination with Sudan III staining, the atherosclerotic lesion formation of both 0.3 and 3 mg/kg groups were markedly reduced compared with control group in both gender (Fig. 1B). About plaque contents, scattered small fibrotic area was distributed in the plaque lesions of both control and telmisartan treatment groups when evaluated by Masson's trichrome staining (Fig. 2). MOMA-2-immunostained area was significantly reduced with telmisartan, but a ratio of positive-stained

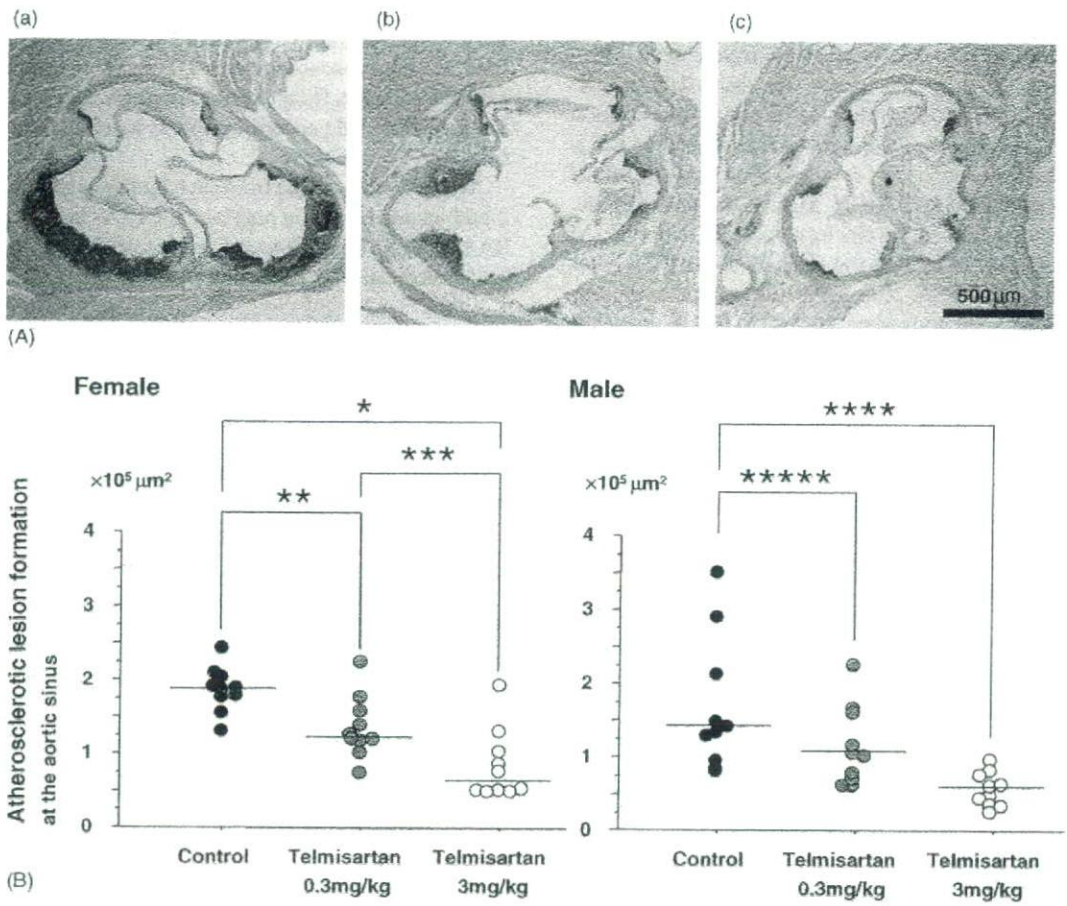

Fig. 1. (A) Representative photographs of atherosclerotic lesion formation at the aortic sinus of each mouse. Panel (a) through (c) are representative photographs of the atherosclerotic lesion formation at the aortic sinus of mice fed a standard chow in control group (a), that treated with 0.3 mg/kg telmisartan (b) and that treated with 3 mg/kg telmisartan (c), respectively. Sections were taken at the same level of aortic sinus and stained with Sudan III staining as described in Section 2. Original magnifications were 40×. A black bar on photomicrograph represents 500 μm. (B) Quantitative analysis of atherosclerotic lesion formation at the aortic sinus in both gender mice. The average lesion area of five sections at the aortic sinus from each mouse was quantified morphometrically as described in Section 2. Each symbol represents the average lesion area in each mouse, with the mean per group indicated by a horizontal line. After 12 weeks telmisartan treatment, the atherosclerotic lesion formation was significantly reduced in both 0.3 and 3 mg/kg telmisartan groups compared with control ($n = 10$ per group). $^{*}P < 0.0001$ vs. control; $^{**}P < 0.01$ vs. control; $^{***}P < 0.01$ vs. telmisartan 0.3 mg/kg; $^{****}P < 0.001$ vs. control; $^{*****}P < 0.05$ vs. control.

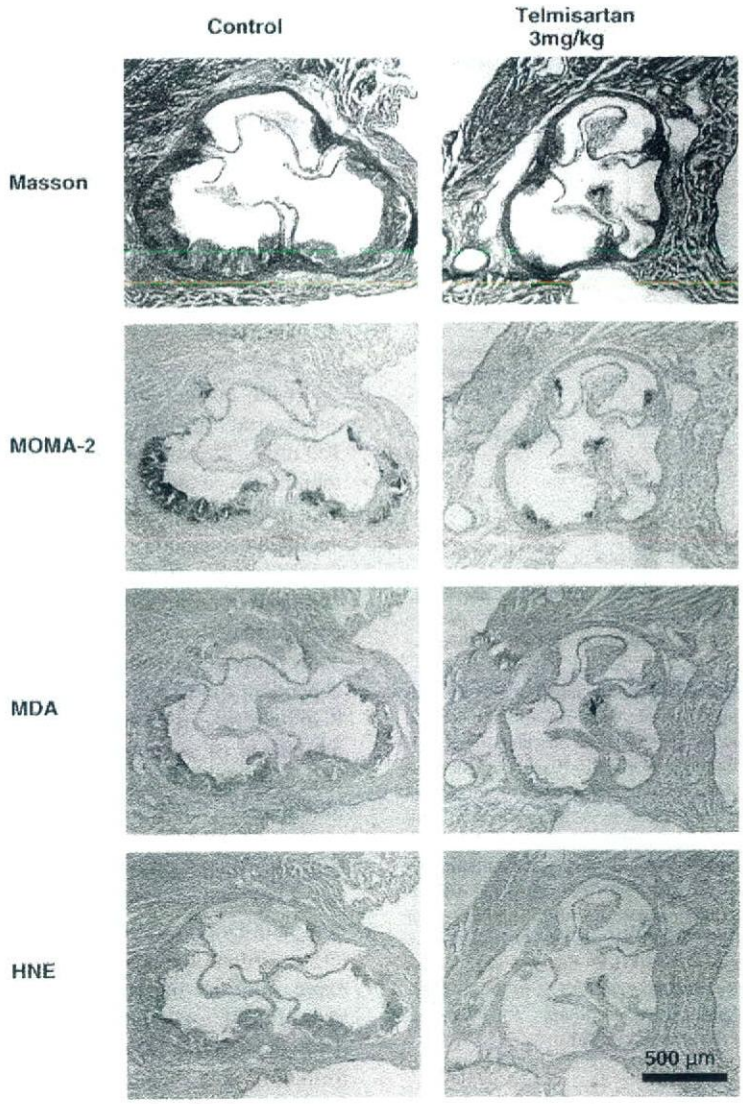

Fig. 2. Effect of telmisartan on plaque contents and the distribution of oxidative stress in atherosclerotic lesion at the aortic sinus. Panels are representative photographs of Masson trichrome staining and immunostained with MOMA-2, MDA and HNE in the atherosclerotic lesions from control group and 3 mg/kg telmisartan group (original magnification were 40×). Scattered fibrosis was partly distributed in the plaque lesions of both groups. On the whole, telmisartan reduced MOMA-2-, MDA- and HNE-immunostained areas compared with control group. A black bar on photomicrograph represents 500 μm.

area to total plaque area was not significantly different among three groups (data not shown). MDA-, HNE-immunostained areas were also reduced with telmisartan (Fig. 2).

3.3. Superoxide production from aortas

To investigate the effect of telmisartan on superoxide production in the aortic vessel wall, we measured superoxide production using the lucigenin-enhanced CL. By treatment with 0.3 and 3 mg/kg telmisartan, superoxide production was significantly decreased compared with control group (Fig. 3A).

3.4. NAD(P)H dependent oxidase activity of aorta homogenates

NAD(P)H dependent oxidase activity in aorta homogenates stimulated with 100 μM NADH or 100 μM NADPH was measured by use of the lucigenin-enhanced CL. Telmisartan significantly decreased NAD(P)H dependent oxidase activity by more than 60% in both 3 and 0.3 mg/kg groups compared with control group (Fig. 3B). Furthermore, aorta homogenates were incubated with either 100 μM DPI or 500 μM apocynin for 15 min to abolish the increment of NAD(P)H dependent oxidase activity. The addition of NAD(P)H oxidase inhibitors significantly reduced

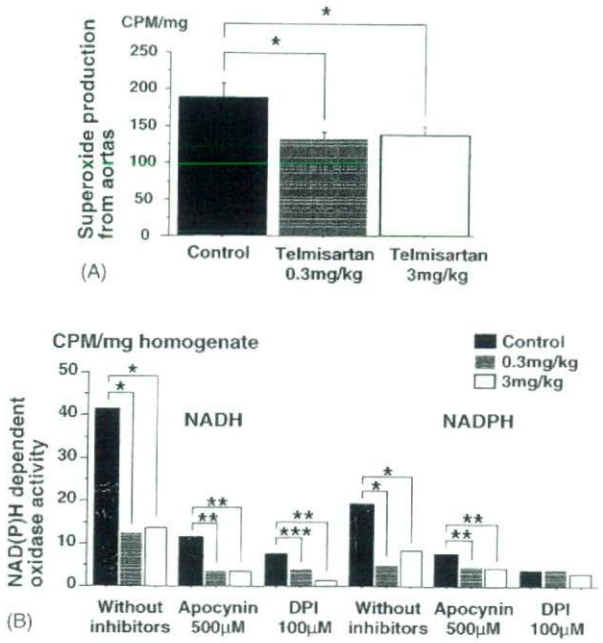

Fig. 3. (A) Effect of telmisartan on superoxide production from whole aortas using lucigenin-enhanced chemiluminescence. Aortic rings were incubated with the Cu–Zn superoxide dismutase inhibitor and vascular superoxide levels were measured by chemiluminescence with 10 μM lucigenin as described in Section 2. The counts by a luminometer were corrected by vessel dry weights. Results were expressed as mean ± S.E.M. ($n = 8$ per group). $^{*}P < 0.05$ vs. control. (B) Effect of telmisartan on NAD(P)H dependent oxidase activity of aorta homogenates using lucigenin-enhanced chemiluminescence. Aorta was homogenated and vascular NAD(P)H dependent oxidase activity was measured by use of chemiluminescence with 250 μM lucigenin in the presence of 100 μM NAD(P)H. NAD(P)H dependent oxidase activity was measured with 500 μM apocynin or 100 μM diphenylene iodinium (DPI) as described in Section 2. Results are expressed as mean ± S.E.M. of counts by luminometer in each group ($n = 8$ per group). $^{*}P < 0.0001$ vs. control; $^{**}P < 0.001$ vs. control; $^{***}P < 0.05$ vs. control.

lucigenin-enhanced CL in both control and telmisartan treatment groups.

3.5. In situ superoxide production in the vessel wall of aorta

In situ superoxide production was measured using DHE oxidative fluorescent microtopography. Ethidium fluorescence was detected throughout all layers of the vessel wall and both doses (0.3 and 3 mg/kg) of telmisartan significantly suppressed the staining (Fig. 4A). We next focused on the vascular superoxide production in the endothelial cells by measuring the ethidium fluorescence particularly on the luminal side of the internal elastic lamina. Endothelial ethidium fluorescence in 0.3 mg/kg group was decreased by 30% compared with control group and by 40% in 3 mg/kg group (Fig. 4B). These results indicated that telmisartan decreased superoxide production from the vessel wall, particularly from endothelial cells.

3.6. 8-iso-PGF2α and SAA levels

8-*iso*-PGF2α level was measured as an indicative marker of systemic oxidative stress. 8-*iso*-PGF2α levels from both urine (Fig. 5A) and plasma samples (Fig. 5B) were significantly decreased with telmisartan treatment compared with control group. On the other hand, SAA levels did not change by telmisartan (Fig. 5C).

4. Discussion

In the present study, we demonstrated that telmisartan suppressed the atherosclerotic lesion formation in apoE-KO mice. The suppressive effect was detected by 0.3 mg/kg telmisartan, which did not change systolic blood pressure, and further suppression occurred by 3 mg/kg telmisartan. As the mechanism of the drug's anti-atherogenic action, we focused on the effects for oxidative states in vivo and in vitro. Telmisartan reduced MDA- and HNE-immunostained areas compared with control group. Telmisartan suppressed superoxide production from the vessel wall via reducing NAD(P)H dependent oxidase activity. Telmisartan also reduced 8-*iso*-PGF2α levels in urine and plasma samples, which are one of indices of systemic oxidative stress. These inhibitory effects on oxidative stress were associated with suppression of atherosclerotic lesion formation.

Several animal studies demonstrated that ARB showed anti-atherogenic effects besides its effect on blood pressure [10–13]. Our finding is in agreement with the results of Hayak et al. and Dol et al., in which ARB reduced atherosclerotic lesion formation in apoE-KO mice via decreased chemokine expression and macrophage accumulation, and the inhibition of LDL oxidation [11,12]. In the present study, we demonstrated that telmisartan reduced atherosclerotic lesion formation in association with the suppression of oxidative stress via the inhibition of NAD(P)H oxidase activity.

Ang II stimulation has been reported to produce ROS from various vascular cell types [2–4]. ROS from the vessel wall are thought to play critical roles in atherogenesis. ROS induce the expression of adhesion molecules and chemokines, accelerate the formation of atherosclerotic plaque, increase matrix metalloprotease production and cause the vulnerable changes of fibrous cap [20].

In the present study, we clearly demonstrated that telmisartan suppressed superoxide production from the vessel wall assessed by lucigenin-enhanced CL method. This action was independent of the blood pressure lowering effect. We also revealed the inhibitory action of telmisartan on superoxide production by DHE staining. Telmisartan suppressed superoxide signals in all layers of aortas, particularly in the endothelium. We next focused on NAD(P)H oxidase to clarify the mechanisms of suppression of superoxide production. Superoxide anion is produced via the activation of NAD(P)H oxidase in vessel wall cells and plays an important role as the intracellular transmission factor in the Ang

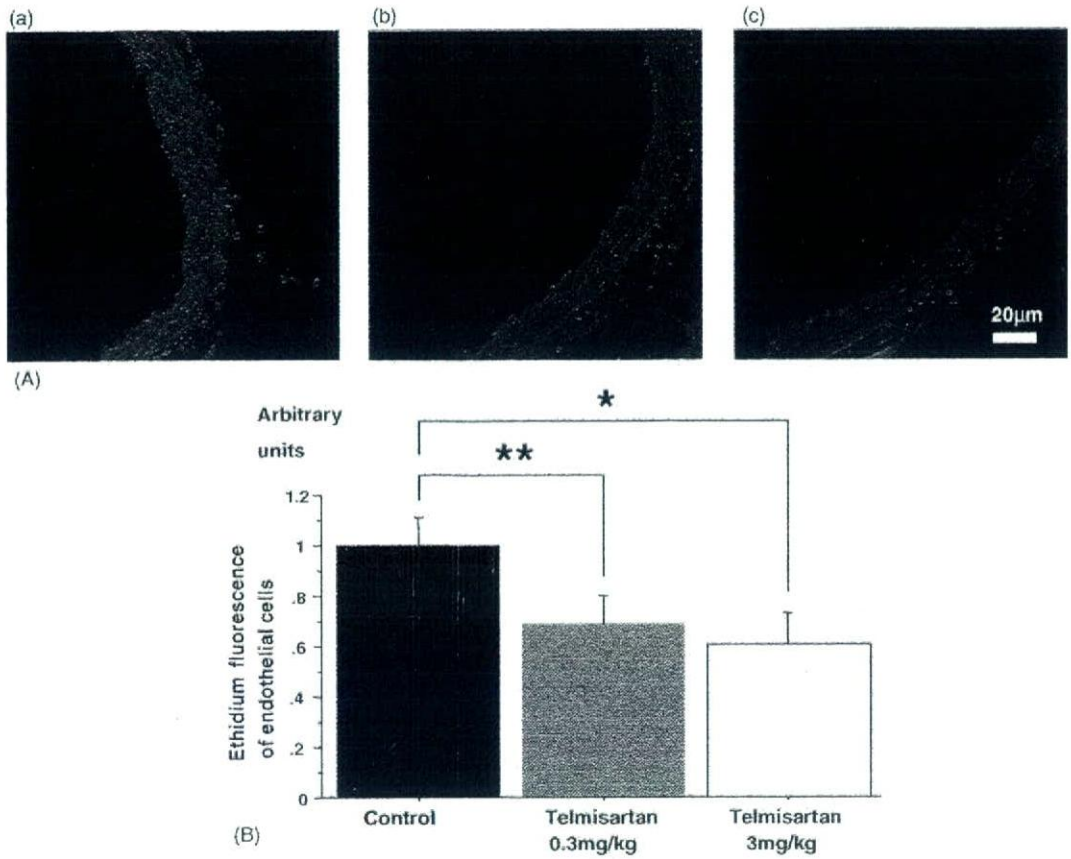

Fig. 4. (A) Representative photographs of in situ superoxide production in aortic vessel wall using dihydroethidium staining. Panel (a) through (c) are representative photographs of aortic vessel wall from each mouse in control group (a), that treated with 0.3 mg/kg telmisartan (b) and that treated with 3 mg/kg telmisartan (c), respectively. Sections were stained with dihydroethidium as described in Section 2. Original magnification were 200×. A white bar represents 20 μm. (B) Quantitative analysis of in situ superoxide production in aorta endothelial cells using dihydroethidium staining. For quantification of ethidium fluorescence from the endothelial cells in high-power (200×) images, fluorescence (intensity × area) was measured only on the luminal side of the internal elastic lamina using the Image J as described in Section 2 and expressed in arbitrary units. Results were expressed as mean ± S.E.M. in each group ($n = 10$ per group). $^{*}P < 0.05$ vs. control; $^{**}P = 0.07$ vs. control.

II-signaling system [21]. Ang II-mediated hypertension is associated with the increased superoxide production and NAD(P)H oxidase activity [7]. Other than hypertension, the increased superoxide production due to NAD(P)H oxidase activation was demonstrated in the rabbit model of atherosclerosis [22]. We examined lucigenin-enhanced CL with NAD(P)H as the substrates and revealed that telmisartan suppressed NAD(P)H dependent oxidase activity with the dosage that did not change blood pressure. This effect was reduced by DPI, an inhibitor of all flavoenzymes and also by apocynin, a more specific inhibitor for NAD(P)H oxidase. These results indicated that the increment of superoxide production was reduced by inactivation of NAD(P)H dependent oxidase activity due to Ang II type 1 receptor blockade with telmisartan.

Our findings are in accordance with the study of Warnholtz et al., who showed that Bay 10-6734, an ARB, reduced plaque formation in association with reductions of vascular superoxide production and NAD(P)H oxidase activity in the rabbit model of atherosclerosis [22]. They did not show whether the anti-atherogenic effects of Bay 10-6734 were independent of the blood pressure lowering effect. In the present study, we clearly demonstrated that telmisartan, a clinically used ARB, reduced atherosclerotic lesion formation without changing blood pressure in apoE-KO mice. In most animal studies showing the blood pressure-independent anti-atherogenic actions of ARB, the far-high dosages have been used compared with those applied clinically [10–13]. In the present study, we showed that the anti-atherogenic action of telmisartan was detected with 0.3 mg/kg, which is lower than the clinically relevant dose. We also showed that telmisartan reduced not only vascular superoxide production but also the marker of systemic oxidative status. 8-*iso*-PGF2α has been recognized as a marker of systemic oxidative stress [23] and revealed as a risk marker in patients with coronary heart disease in matched case-control studies [24]. In this study, telmisartan suppressed 8-*iso*-PGF2α levels in both urine and plasma with the non-blood pressure lowing dosage.

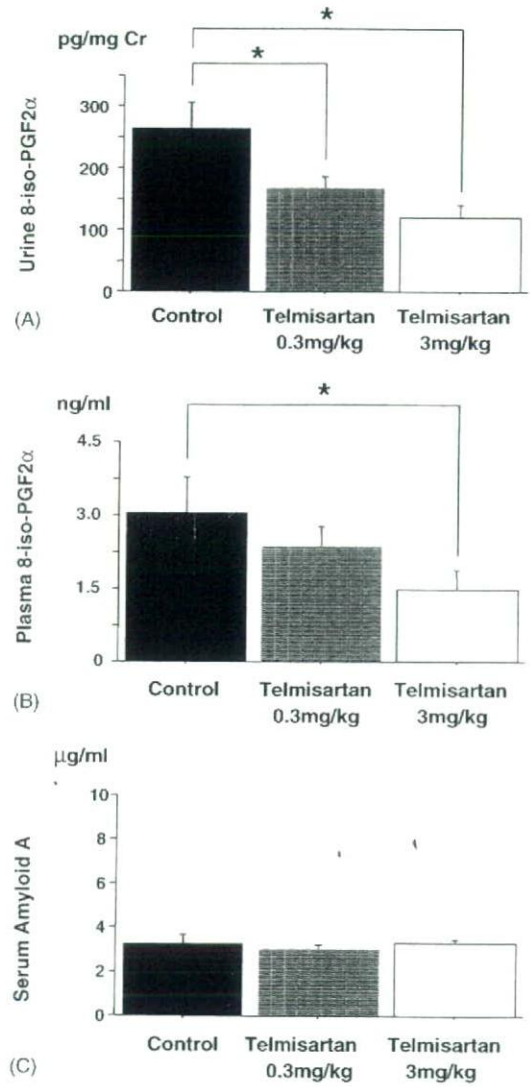

Fig. 5. (A) and (B) Effect of telmisartan on 8-*iso*-PGF2α levels of urine and plasma samples 8-*iso*-PGF2α from urine (A) and plasma (B) samples were measured as described in Section 2. Urine data are corrected by urine creatinine levels. Results were expressed as mean ± S.E.M. ($n = 8$ per group). $^{*}P < 0.05$ vs. control. (C) Effect of telmisartan on SAA levels. SAA levels were measured as described in Section 2. Results were expressed as mean ± S.E.M. ($n = 8$ per group).

The association of suppressed oxidative stress and reduction of atherosclerotic lesion formation does not necessarily mean the cause-effect relation. Both occurred independently of changes in blood pressure, and the well-known roles of oxidative stress in the initiation and progression of atherosclerosis strongly suggest that the anti-oxidative effects are at least partly responsible for the suppression of atherosclerotic lesion formation by telmisartan. Telmisartan might, however, reduce atherosclerotic lesion size by mechanisms other than its effects on oxidative stress, such as anti-inflammatory effects and effects on peroxisome proliferator-activated receptor-gamma (PPAR-g) activity. It is reported that telmisartan induced PPAR-g activation [25,26], but in the present study, telmisartan did not change plasma glucose, triglyceride or insulin levels. Therefore the effect of telmisartan on PPAR-g seemed to play a minimum role in the present study. Further, Ang II increases expression of lectin-like oxidized LDL receptor of macrophage and accelerates the foam cell formation and the deposition of oxidized lipid to the plaque [27]. Further studies are needed to clarify how inhibition of those actions of Ang II by telmisartan is related to its anti-atherogenic action.

As a limitation of the present study, we quantified superoxide production from aorta homogenates by use of 250 μm lucigenin. The validity of data on superoxide has been questioned when the relatively high dose of lucigenin is applied. In the present study, however, the levels of oxidative stress were relatively low, and we could not detect any fluorescence signals when we used 5 μm lucigenin, which was revealed not to produce superoxide by itself. In the report of Warnholtz et al., they compared the data on superoxide productions measured by 5 μM lucigenin with those by 250 μM lucigenin and confirmed the validity of the data obtained by the latter concentration [22].

In conclusion, we for the first time reported that in apoE-KO mice clinically relevant doses of telmisartan reduced atherosclerosis in association with suppressions in vascular oxidative stress and vascular systemic oxidative state. Our results suggest that telmisartan is beneficial not only for hypertension but also for atherosclerosis and imply that this drug may work as an anti-oxidant in various organs, although additional experiments will be needed.

References

[1] Daugherty A, Cassis L. Chronic angiotensin II infusion promotes atherogenesis in low density lipoprotein receptor −/− mice. Ann NY Acad Sci 1999;892:108–18.
[2] Zhang H, Schmeisser A, Garlichs CD, et al. Angiotensin II-induced superoxide anion generation in human vascular endothelial cells: role of membrane-bound NADH/NADPH-oxidases. Cardiovasc Res 1999;44:215–22.
[3] Sorescu D, Weiss D, Lassegue B, et al. Superoxide production and expression of nox family proteins in human atherosclerosis. Circulation 2002;105:1429–35.
[4] Cathcart MK. Regulation of superoxide anion production by NADPH oxidase in monocytes/macrophages: contributions to atherosclerosis. Arterioscler Thromb Vasc Biol 2004;24:23–8.
[5] Diet F, Pratt RE, Berry GJ, Momose N, Gibbons GH, Dzau VJ. Increased accumulation of tissue ACE in human atherosclerotic coronary artery disease. Circulation 1996;94:2756–67.
[6] Yang BC, Phillips MI, Mohuczy D, et al. Increased angiotensin II type 1 receptor expression in hypercholesterolemic atherosclerosis in rabbits. Arterioscler Thromb Vasc Biol 1998;18:1433–9.
[7] Rajagopalan S, Kurz S, Munzel T, et al. Angiotensin II-mediated hypertension in the rat increases vascular superoxide production via membrane NADH/NADPH oxidase activation. Contribution to alterations of vasomotor tone. J Clin Invest 1996;97:1916–23.
[8] Chen XL, Tummala PE, Olbrych MT, Alexander RW, Medford RM. Angiotensin II induces monocyte chemoattractant protein-1 gene expression in rat vascular smooth muscle cells. Circ Res 1998;83:952–9.

[9] Tummala PE, Chen XL, Sundell CL, et al. Angiotensin II induces vascular cell adhesion molecule-1 expression in rat vasculature: a potential link between the renin-angiotensin system and atherosclerosis. Circulation 1999;100:1223–9.
[10] Strawn WB, Chappell MC, Dean RH, Kivlighn S, Ferrario CM. Inhibition of early atherogenesis by losartan in monkeys with diet-induced hypercholesterolemia. Circulation 2000;101:1586–93.
[11] Hayek T, Attias J, Coleman R, et al. The angiotensin-converting enzyme inhibitor, fosinopril, and the angiotensin II receptor antagonist, losartan, inhibit LDL oxidation and attenuate atherosclerosis independent of lowering blood pressure in apolipoprotein E-deficient mice. Cardiovasc Res 1999;44:579–87.
[12] Dol F, Martin G, Staels B, et al. Angiotensin AT1 receptor antagonist in apolipoprotein E-deficient mice. J Cardiovasc Pharmacol 2001;38:395–405.
[13] Takai S, Kim S, Sakonjo H, Miyazaki M. Mechanisms of angiotensin II type 1 receptor blocker for anti-atherosclerotic effect in monkeys fed a high-cholesterol diet. J Hypertens 2003;21:361–9.
[14] Paigen B, Morrow A, Holmes PA, Mitchell D, Williams RA. Quantitative assessment of atherosclerotic lesions in mice. Atherosclerosis 1987;68:231–40.
[15] Ozaki M, Kawashima S, Yamashita T, et al. Overexpression of endothelial nitric oxide synthase accelerates atherosclerotic lesion formation in apoE-deficient mice. J Clin Invest 2002;110:331–40.
[16] Bradford MM. A rapid and sensitive method for the quantification of microgram quantities of protein utilizing the principle of protein-dye binding. Anal Biochem 1972;72:248–54.
[17] Munzel T, Kurz S, Rajagopalan S, et al. Hydralazine prevents nitroglycerin tolerance by inhibiting activation of a membrane-bound NADH oxidase: a new action for an old drug. J Clin Invest 1996;98:1465–70.
[18] Miller FJ, Gutterman DD, Rios CD, Heistad DD, Davidson BL. Superoxide production in vascular smooth muscle contributes to oxidative stress and impaired relaxation in atherosclerosis. Circ Res 1998;82:1298–305.
[19] Alp NJ, Mussa S, Khoo J, et al. Tetrahydrobiopterin-dependent preservation of nitric oxide-mediated endothelial function in diabetes by targeted transgenic GTP-cyclohydrolase I overexpression. J Clin Invest 2003;112:725–35.
[20] Rajagopalan S, Meng XP, Ramasamy S, Harrison DG, Galis ZS. Reactive oxygen species produced by macrophage-derived foam cells regulate the activity of vascular matrix metalloproteinases in vitro. Implications for atherosclerotic plaque stability. J Clin Invest 1996;98:2572–9.
[21] Cai H, Harrison DG. Endothelial dysfunction in cardiovascular diseases: the role of oxidative stress. Circ Res 2000;87:840–4.
[22] Warnholtz A, Nickenig G, Schulz E, et al. Increased NADH-oxidase-mediated superoxide production in the early stages of atherosclerosis: evidence for involvement of the renin-angiotensin system. Circulation 1999;99:2027–33.
[23] Pratico D, Tangirala RK, Rader DJ, Rokach J, FitzGerald GA. Vitamin E suppresses isoprostane generation in vivo and reduces atherosclerosis in ApoE-deficient mice. Nat Med 1998;4:1189–92.
[24] Schwedhelm E, Bartling A, Lenzen H, et al. Urinary 8-*iso*-prostaglandin F2alpha as a risk marker in patients with coronary heart disease: a matched case-control study. Circulation 2004;109:843–8.
[25] Schupp M, Janke J, Clasen R, Unger T, Kintscher U. Angiotensin type 1 receptor blockers induce peroxisome proliferator-activated receptor-gamma activity. Circulation 2004;109:2054–7.
[26] Benson SC, Pershadsingh HA, Ho CI, et al. Identification of telmisartan as a unique angiotensin II receptor antagonist with selective PPAR gamma-modulating activity. Hypertension 2004;43:993–1002.
[27] Sawamura T, Kume N, Aoyama T, et al. An endothelial receptor for oxidized low-density lipoprotein. Nature 1997;386:73–7.